



UNIVERSITY
OF WOLLONGONG
AUSTRALIA

University of Wollongong
Research Online

Faculty of Engineering and Information Sciences -
Papers: Part A

Faculty of Engineering and Information Sciences

2015

Fractional order modelling of the cumulative deformation of granular soils under cyclic loading

Yifei Sun

University of Wollongong, ys910@uowmail.edu.au

Yang Xiao

Chongqing University, hhxyanson@163.com

Khairul Fikry Hanif

University of Western Australia

Publication Details

Sun, Y., Xiao, Y. & Hanif, K. Fikry. (2015). Fractional order modelling of the cumulative deformation of granular soils under cyclic loading. *Acta Mechanica Solida Sinica*, 28 (6), 647-658.

Research Online is the open access institutional repository for the University of Wollongong. For further information contact the UOW Library:
research-pubs@uow.edu.au

Fractional order modelling of the cumulative deformation of granular soils under cyclic loading

Abstract

To model the cumulative deformation of granular soils under cyclic loading, a mathematical model was proposed. The power law connection between the shear strain and loading cycle was represented by using fractional derivative approach. The volumetric strain was characterized by a modified cyclic flow rule which considered the effect of particle breakage. All model parameters were obtained by the cyclic and static triaxial tests. Predictions of the test results were provided to validate the proposed model. Comparison with an existing cumulative model was also made to show the advantage of the proposed model.

Disciplines

Engineering | Science and Technology Studies

Publication Details

Sun, Y., Xiao, Y. & Hanif, K. Fikry. (2015). Fractional order modelling of the cumulative deformation of granular soils under cyclic loading. *Acta Mechanica Solida Sinica*, 28 (6), 647-658.

FRACTIONAL ORDER MODELLING OF THE CUMULATIVE DEFORMATION OF GRANULAR SOILS UNDER CYCLIC LOADING

Yifei Sun¹, Yang Xiao², Khairul Fikry Hanif³

1. Institute for Mathematics and its Applications, University of Wollongong, Wollongong 2522, Australia

2. College of Civil Engineering, Chongqing University, Chongqing 400045, China

2. Faculty of Engineering, Computing and Mathematics, University of Western Australia, Perth 6907, Australia

ABSTRACT: To model the cumulative deformation of granular soils under cyclic loading, a mathematical model is proposed. The power law connection between the shear strain and loading cycle is represented by using fractional derivative approach. The volumetric strain is characterized by a modified cyclic flow rule which considers the effect of particle breakage. All model parameters can be obtained by the cyclic and static triaxial tests. Predictions of the test results are provided to validate the proposed model. Comparison with an existing cumulative model is also performed to show the advantage of the proposed model.

KEY WORDS: cumulative deformation; cyclic stress; cyclic flow rule; fractional derivative; granular soil

I. INTRODUCTION

Well-constructed infrastructure could still suffer differential foundation settlements and structural damages if they were exposed to continuous cyclic loadings induced by traffics, construction activities and even sea waves, etc. If the number of loading cycles is sufficiently large then even relatively small strain amplitudes may endanger the serviceability of structures in the long run, especially if their displacement tolerance is small. Miura et al. [1] reported that the additional monitoring settlement of Saga airport road resulted from landing and taking off of aircraft reached about 150 mm in just 2 years. In addition, the tunnel settlement of the Shanghai Metro Line 1 caused by dynamic train loading had reached up to 155 mm in only 4 years [2]. Detailed understanding of the cumulative deformation and failure mechanism of soils under repeated loading with large number of cycles is thus essential for the proper design and maintenance of airport roads, railway tracks and highway pavements, etc. To investigate and constitutive modeling of the cyclic stress strain response of soils, lots of experimental and theoretical studies have been conducted [3-15]. Khalili et al. [7] and Liu et al. [12] studied the cyclic behaviour of gravelly soil under cyclic loading with low frequency. Ishikawa et al. [16] examined the mechanical response of railroad ballast subjected to repeated train passages on ballasted track by using multi-ring shear test. Suiker et al. [17] and Indraratna et al. [18-20] investigated the cyclic behaviour of both ballast and subballast under low and high loading frequency, from which the influences of loading history and confining pressure as well as the loading frequency were observed. These excellent works provide fundamental tools for further understanding the cyclic behaviour of granular soils, which is significant in practical design methods for the stability of both over-

40 ground and underground structures. However, some of the tests only covered a cyclic load
41 with very small loading cycles, say less than 100. The corresponding constitutive models,
42 such as the bounding surface model [7, 21] and the generalized plasticity model [22-23] can
43 only simulate the cyclic behaviour of granular soils for very limited cycles. For the
44 cumulative strain under high loading cycles ($N > 10^3$), these models usually failed due to the
45 unintentional accumulation of numerical errors and the huge calculation effort, especially in
46 the finite element analysis. It is of little possibility for these theoretical models to be used in
47 practical engineering where the loads usually have at least tens of thousands of cycles. To
48 overcome this limitation, lots of empirical and semi-empirical models were proposed. For
49 example, Indraratna et al. [24] proposed a pressure-dependent elastoplastic model by
50 introducing empirical parameters to consider the effect of stress history, stress ratio, number
51 of cycles, and breakage. In fact, the cumulative deformation of granular soils under cyclic
52 stress is not only influenced by the current loading stress but also affected by previous
53 loading cycles. It is indeed a memory-intensive phenomenon which can be mathematically
54 expressed by a simple power law of the loading cycles, N , as suggested by Chrismer and
55 Selig [25] and Indraratna et al. [26], etc. Inspired by the creep of soils under constant static
56 stress, lots of empirical models for predicting cumulative deformation of granular soils, such
57 as sand, ballast and subballast, etc., subjected to averaged cyclic deviator stress were
58 suggested [5-6, 8-11]. Due to the explicit expressions, these models can be easily
59 incorporated in the engineering-oriented finite element method. However, most of the
60 existing models contain a lot of model parameters and even so still cannot well predict the
61 accumulation of residual strain in soils subjected to cyclic loading with many cycles. Most
62 importantly, they did not physically explain the reason for the cumulative deformation of
63 granular soils evolving in a power law. Sun et al. [27-28] suggested the use of fractional
64 calculus in modeling the dependency of power law in complex mechanical process. Later,
65 Yin et al. [29-30] proposed a framework for constitutive modeling the strain hardening and
66 softening of geomaterials under static loading by employing the basic theory of fractional
67 derivative. However, fractional order constitutive modeling of cumulative behaviour of soils
68 under cyclic loading is still rarely reached. The aim of this paper is to make an attempt to
69 model the cumulative shear strain of granular soils subjected to drained cyclic loading based
70 on the theory of fractional derivative. Moreover, a modified cyclic flow rule considering the
71 effect of particle breakage is proposed for determining the corresponding cumulative
72 volumetric strain. Comparison between the experimental results and model predictions is also
73 presented.

74

75 II. CUMULATIVE STRAIN BASED ON FRACTIONAL CALCULUS

76 2.1. General formula

77 To quantify the cyclic behaviour of granular soils, laboratory tests, including the biaxial and
78 triaxial tests are usually conducted under either constant stress rate ($d\sigma$) or constant strain
79 rate ($d\varepsilon$). By regarding the soil as an intermediate material, lying between the ideal solids

80 which obey Hooke' law and the Newtonian fluids which satisfy Newton's law of viscosity,
 81 the stress (σ) and strain (ε) relationship should obey [29]

$$82 \quad \sigma(t) = G \frac{d^\alpha \varepsilon(t)}{dt^\alpha} \quad (1)$$

83 where α denotes the fractional derivative order, ranging between 0 and 1. With α
 84 approaching 1, the material behaves increasingly like an ideal solid, whereas it becomes
 85 increasingly softer like a fluid with α approaching 0. G is a material constant. t denotes the
 86 time for loading and unloading. To start with, the Riemann-Liouville definitions of the
 87 fractional order derivative (Eq. (2)) and integral (Eq. (3)) of function f are used [30]:

$$88 \quad \frac{d^\alpha f}{dt^\alpha} = \frac{1}{\Gamma(1-\alpha)} \frac{d}{dt} \int_0^t \frac{f(\tau)}{(t-\tau)^\alpha} d\tau \quad (2)$$

$$89 \quad \frac{d^{-\alpha} f}{dt^{-\alpha}} = \frac{1}{\Gamma(\alpha)} \int_0^t \frac{f(\tau)}{(t-\tau)^{1-\alpha}} d\tau \quad (3)$$

90 where $\Gamma(\bullet)$ denotes the gamma function and can be formulated as

$$91 \quad \Gamma(t) = \int_0^\infty e^{-\tau} \tau^{t-1} d\tau \quad (4)$$

92 For soils loaded and then unloaded for N cycles, the total strain can be obtained by
 93 summing the strain of each loading and unloading cycle, that is

$$94 \quad \begin{aligned} \varepsilon(t) = & \frac{1}{G_1} \frac{1}{\Gamma(\alpha)} \int_0^T \frac{\sigma(\tau)}{(t-\tau)^{1-\alpha}} d\tau + \frac{1}{G'_1} \frac{1}{\Gamma(\alpha)} \int_{\frac{T}{2}}^T \frac{\hat{\sigma}(\tau)}{(t-\tau)^{1-\alpha}} d\tau \\ & + \frac{1}{G_2} \frac{1}{\Gamma(\alpha)} \int_T^{T+\frac{T}{2}} \frac{\sigma(\tau)}{(t-\tau)^{1-\alpha}} d\tau + \frac{1}{G'_2} \frac{1}{\Gamma(\alpha)} \int_{T+\frac{T}{2}}^{2T} \frac{\hat{\sigma}(\tau)}{(t-\tau)^{1-\alpha}} d\tau \\ & + \dots + \frac{1}{G_N} \frac{1}{\Gamma(\alpha)} \int_{(N-1)T}^{(N-1)T+\frac{T}{2}} \frac{\sigma(\tau)}{(t-\tau)^{1-\alpha}} d\tau + \frac{1}{G'_N} \frac{1}{\Gamma(\alpha)} \int_{(N-1)T+\frac{T}{2}}^{NT} \frac{\hat{\sigma}(\tau)}{(t-\tau)^{1-\alpha}} d\tau \end{aligned} \quad (5)$$

95 where the time, T , denote the loading period for one complete loading and unloading process.
 96 σ and $\hat{\sigma}$ denote the loading and unloading stresses, respectively. G_i and G'_i ($i = 1, 2, 3, \dots,$
 97 N) are the loading and unloading moduli, respectively. Rearranging Eq. (5), one has

$$98 \quad \varepsilon(t) = \sum_{i=1}^N \frac{1}{G_i} \frac{1}{\Gamma(\alpha)} \int_{(i-1)T}^{(i-1)T+\frac{T}{2}} \frac{\sigma(\tau)}{(t-\tau)^{1-\alpha}} d\tau + \sum_{i=1}^N \frac{1}{G'_i} \frac{1}{\Gamma(\alpha)} \int_{(i-1)T+\frac{T}{2}}^{iT} \frac{\hat{\sigma}(\tau)}{(t-\tau)^{1-\alpha}} d\tau \quad (6)$$

99 Following Yin et al. [29], for soils tested under triaxial loading condition, the shear strain
 100 ε_s and volumetric strain can be reformulated by using Eq. (6) as

$$101 \quad \varepsilon_s = \sum_{i=1}^N \frac{1}{G_i} \frac{1}{\Gamma(\alpha)} \int_{(i-1)T}^{(i-1)T+\frac{T}{2}} \frac{q(\tau)}{(t-\tau)^{1-\alpha}} d\tau + \sum_{i=1}^N \frac{1}{G'_i} \frac{1}{\Gamma(\alpha)} \int_{(i-1)T+\frac{T}{2}}^{iT} \frac{\hat{q}(\tau)}{(t-\tau)^{1-\alpha}} d\tau \quad (7a)$$

$$\varepsilon_v = \sum_{i=1}^N \frac{1}{K_i} \frac{1}{\Gamma(\alpha)} \int_{(i-1)T}^{(i-1)T+\frac{T}{2}} \frac{p'(\tau)}{(t-\tau)^{1-\alpha}} d\tau + \sum_{i=1}^N \frac{1}{K'_i} \frac{1}{\Gamma(\alpha)} \int_{(i-1)T+\frac{T}{2}}^{iT} \frac{\hat{p}'(\tau)}{(t-\tau)^{1-\alpha}} d\tau \quad (7a)$$

where $\varepsilon_s = 2/3(\varepsilon_1 - \varepsilon_3)$ and $\varepsilon_v = (\varepsilon_1 + 2\varepsilon_3)$; ε_1 and ε_3 are the first and third principal strains, respectively. $q (= \sigma'_1 - \sigma'_3)$ and $p' (= \sigma'_1 + 2\sigma'_3)/3$ are the loading deviator and mean effective principal stresses, respectively; σ'_1 and σ'_3 are the first and third effective principal stresses, respectively. \hat{q} denote the unloading deviator stresses. K_i and K'_i ($i = 1, 2, 3, \dots, N$) are the volumetric loading and unloading moduli, respectively. Note that $dq = d\sigma'_1$ and $dp' = d\sigma'_1/3$ during loading and $d\hat{q} = -d\sigma'_1$ and $d\hat{p}' = -d\sigma'_1/3$ during unloading.

2.2 Formula for long-term deformation

It is noted that Eq. (6) strictly counts the strain variation of each individual loading cycle. The entire iteration steps may cause huge calculation effort and numerical errors if large amounts of loading cycles are involved. Therefore, a modified fractional order model for long-term cyclic loading needs to be proposed. As adopted by Indraratna et al. [24, 26] as well as Chrismer and Selig [25], the power law connection between the cumulative strain and its corresponding loading cycles can well predict the long-term deformation of granular soils. Most importantly, it can be easily implemented in the finite element analysis because of its explicit expression. To better take into account this power law phenomenon, the fractional derivative is employed here. For cyclic triaxial test as schematically illustrated by Fig. 1, the cumulative shear strain ε_s^p is assumed to result from the average deviator stress q^{av} [5] and have the following relationship:

$$\frac{d^\alpha \varepsilon_s^p}{dN^\alpha} = \frac{1}{rp_a} q^{av} \quad (8)$$

where the shear strain ε_s^p is fractionally differentiated by the number of loading cycles (N) instead of the time t . This is because in the context of cyclic loading rate means a derivative with respect to the number, N . It should be noted that the number of load cycles, N , can be related to the real loading time, t , by using $t = N / f$ where f denotes the load frequency. Similar approaches can be found elsewhere in [6, 8-10]. r is the shear-related parameter, reflecting the long-term behavior of granular soils. p_a is the atmospheric pressure (101kPa), for the purpose of parameter dimensionless. Applying Laplace and inverse Laplace transformations to both sides of Eq. (8), yields

$$d\varepsilon_s^p = \frac{\alpha q^{av}}{\Gamma(1+\alpha)rp_a} N^{\alpha-1} \quad (9)$$

Eq. (9) is the ultimate correlation between the cumulative strain ε_s and the loading cycles, N . It offers mathematical representation for how the cumulative strain frequently manifests itself through the empirical formula with the form of a power-law function.

134

135

III. CYCLIC FLOW RULE

136 Based on the principle of energy conservation, many different kinds of functions [32-34]
 137 describing the static flow for various geomaterials have been deduced, for instance, the Rowe
 138 dilatancy equation [32]. However, for granular soils which not only experience particle
 139 arrangement but also particle breakage during loading [35]. The energy dissipated by particle
 140 breakage for one individual loading process is assumed to be proportional to the energy
 141 dissipated by particle arrangement as suggested by McDowell [36]. Therefore, the following
 142 energy conservative equation is used:

$$143 \quad qd\varepsilon_s^p + p'd\varepsilon_v^p = Mp'd\varepsilon_s^p + Mp'd\varepsilon_s^p \frac{M^a - \eta^a}{\eta^a} \quad (10)$$

144 where p' ($= \sigma'_1/3 + 2\sigma'_3/3$) is the mean effective principal stress. The stress ratio $\eta = q/p'$.
 145 M ($= M_0 p'^b$) is the critical state friction parameter of the tested material. M_0 and b are the
 146 material constants. It was found that the shear and volumetric strains of soils tested under
 147 cyclic loading flows according to a cyclic flow rule [6, 8]. Wichtmann et al. [8-10] proposed
 148 a stress dilatancy equation by assuming that the energy was only dissipated by particle
 149 slippage. However, as stated before, granular soils not only suffer particle arrangement but
 150 also breakage during loading. Therefore, to better reflect the deformation mechanism, a
 151 modified cyclic flow rule is suggested here by considering energy dissipation from both
 152 particle rearrangement and breakage. For an arbitrary cyclic loading process, the total plastic
 153 strain for the tested sample can be expressed as an integral of all the increments in Eq. (10).

$$154 \quad \int d\varepsilon_v^p = M^{a+1} \int \frac{1}{\eta^a} d\varepsilon_s^p - \int \eta d\varepsilon_s^p \quad (11)$$

155 The stress ratio, η , in Eq. (11) varies with time. However, it can be treated as a mean value,
 156 η_m , as suggested by Chang and Wichtmann [37].

$$157 \quad \eta_m = \frac{\int \eta d\varepsilon_s^p}{\int d\varepsilon_s^p} \quad (12)$$

$$158 \quad \eta_m^{-a} = \frac{\int \eta^{-a} d\varepsilon_s^p}{\int d\varepsilon_s^p} \quad (13)$$

159 Substituting Eqs. (12) and (13) into Eq. (11), one has

$$160 \quad \int d\varepsilon_v^p = \frac{M^{a+1} - \eta_m^{a+1}}{\eta_m^a} \int d\varepsilon_s^p \quad (14)$$

161 By rearranging Eq. (14), the relationship between the cumulative volumetric strain and the
 162 the shear strain can be obtained as

$$163 \quad \frac{d\varepsilon_v^p}{d\varepsilon_s^p} \approx \frac{M^{a+1} - \eta_m^{a+1}}{\eta_m^a} \quad (15)$$

164 Eq. (15) can be regarded as a modified cyclic flow rule for granular soils considering the
 165 influence of particle breakage. However, the value of the stress ratio, η_m , needs to be
 166 determined before the actual use of Eq. (15) in capturing the flow direction of the cumulative
 167 strains in granular soils. According to the laboratory observation by Chang and Wichtmann
 168 [37], η_m is slightly larger than the averaged stress ratio, η^{av} , in cyclic loading. Therefore, the
 169 averaged stress ratio, η^{av} , is used instead of the mean value, η_m .

$$170 \quad \frac{d\varepsilon_v^p}{d\varepsilon_s^p} = \frac{M^{a+1} - (\eta^{av})^{a+1}}{\beta(\eta^{av})^a} \quad (16)$$

171 where β is the material constant, diminishing the influence of the difference between the
 172 mean stress ratio, η_m , and the averaged stress ratio, η^{av} , on the cyclic flow direction. Fig. 2
 173 shows the comparison of the flow directions predicted by Eq. (16) and the modified Cam-
 174 clay model suggested by Wichtmann et al. [9, 38]. The modified cyclic flow rule takes into
 175 account the effect of particle breakage and thus gives better performance than that by
 176 Wichtmann et al. [38], especially in the stress dilatant part where the trend of volumetric
 177 dilation was reduced by the particle breakage occurred inside the sample.

178

179 IV. CONSTITUTIVE EQUATIONS

180 The cumulative total strain is a sum of the elastic strain and the plastic strain, which can be
 181 formulated as

$$182 \quad d\varepsilon_v = d\varepsilon_v^e + d\varepsilon_v^p \quad (17)$$

$$183 \quad d\varepsilon_s = d\varepsilon_s^e + d\varepsilon_s^p \quad (18)$$

184 where ε_v^e and ε_s^e are the resilient volumetric and shear strains, respectively. The resilient
 185 parts of the total strains can be given as

$$186 \quad d\varepsilon_v^e = \frac{dp^{av}}{K} \quad (19)$$

$$187 \quad d\varepsilon_s^e = \frac{q^{av}}{3G} \quad (20)$$

188 where the shear modulus G can be defined as [39-40]

$$189 \quad G = G_0 \frac{(2.97 - e_0)^2}{1 + e_0} \sqrt{p^{\text{av}} p_a} \quad (21)$$

190 where e_0 is the initial void ratio of the sample. $P_a = 101$ kPa, is the atmospheric pressure. G_0
191 denotes the shear-related modulus for virgin loading; K is the bulk modulus that is expressed
192 as

$$193 \quad K = K_0 \frac{(2.97 - e_0)^2}{1 + e_0} \sqrt{p^{\text{av}} p_a} \quad (22)$$

194 where K_0 denotes the compression-related modulus for virgin loading;. The cumulative
195 plastic strains caused by cyclic loading can be given as

$$196 \quad d\varepsilon_s^p = \frac{\alpha q^{\text{av}}}{\Gamma(1 + \alpha) r p_a} N^{\alpha-1} \quad (23)$$

$$197 \quad d\varepsilon_s^p = \frac{M^{a+1} - (\eta^{\text{av}})^{a+1}}{\beta (\eta^{\text{av}})^a} \frac{\alpha q^{\text{av}}}{\Gamma(1 + \alpha) r p_a} N^{\alpha-1} \quad (24)$$

198 where parameter r should depend not only on the soil type but also on the stress state and
199 initial physical state. As suggested by Li et al. [41], it was not convenient to introduce the
200 moisture content and dry density directly into the equation. However, the cyclic strain
201 amplitude of the first loading cycle can indirectly represent the influence of the initial
202 physical state on the cumulative strain of the granular soils. Thus, an empirical formula
203 considering the influence of both stress state and initial physical state of soils is suggested as

$$204 \quad r = D (\eta^{\text{av}})^m (\varepsilon^{\text{ampl}})^n \quad (25)$$

205 where D , m , n , are material constants and the cyclic strain amplitude, $\varepsilon^{\text{ampl}}$, can be obtained
206 by using

$$207 \quad \varepsilon^{\text{ampl}} = \frac{\Delta q}{G} \frac{1}{1 - \frac{2\Delta q}{\Delta q_{\text{max}}}} \quad (26)$$

208 where Δq and Δq_{max} denote the cyclic amplitude of the deviator stress and the distance away
209 from the failure envelop, respectively, as illustrated in Fig. 1. Note that $\Delta p'$ and p^{av} in Fig. 1
210 are the cyclic amplitude of the mean principal stress and the averaged mean principal stress,
211 respectively.

212

213

V. MODEL PARAMETERS

214 This model contains ten parameters, i.e., G_0 , ν , M_0 , a , b , α , β , D , m and n . All of them
 215 can be determined by static and cyclic triaxial tests. The moduli K_0 and G_0 can be obtained by
 216 resonant column test or measuring the initial stress-strain of the sample subjected to triaxial
 217 loading. The critical state friction parameter M_0 and b related to the gradient of the critical
 218 state stress in the p - q space and can be obtained by static triaxial test. The critical state stress
 219 along with the peak stress envelop of railroad ballast, as shown in Fig. 3 varies with the initial
 220 confining pressures which is different from that of sand [42-43]. This can be partially
 221 attributed to the particle breakage during sample preparation which changed the initial
 222 particle size distribution of the railroad ballast. The critical stress ratio, M , depends on the
 223 effective mean principal stress [43-45]. An increase of stress level leads to an increase of the
 224 particle breakage [46-48]. Therefore, a varying critical stress ratio as suggested by Xiao et al.
 225 [43] is used. However, the critical state friction angle for sand [10] is taken as constant here.
 226 Parameters a and β define the flow direction of sand under cyclic loading and can be
 227 determined by adjusting the value of β to obtain a better correlation between
 228 $\ln(d\varepsilon_v^p / d\varepsilon_s^p + \eta^{av} / \beta)$ and $\ln(\eta^{av})$, where the value of a can be obtained by measuring the
 229 slope of the corresponding fitting line, as illustrated in Fig. 4. The fractional derivative order,
 230 α , describes the rate of strain accumulation and is independent of the deviator stress
 231 according to the research by Li et al. [41]. Therefore, it can be determined by fitting the
 232 relationship between the shear strain, ε_s^p , and the number of loading cycles, N . Note that
 233 sometimes the cumulative strain used to calculate the exponent, α , as illustrated in Fig. 5, is
 234 the cumulative total strain rather than the cumulative plastic strain. This is considered
 235 acceptable because the resilient/elastic strain will become nearly constant and negligible
 236 when compared with the plastic strain after a certain number of loading cycles. Parameters D ,
 237 m , and n can be obtained by regression with the value of r (Fig. 6) which is related to the
 238 plastic strain of the first loading cycle. To show the advantage of the present model in
 239 simulating the cumulative deformation, the prediction of the mathematical model proposed
 240 by François et al. [46] is also provided for comparison. The model contains 10 parameters
 241 (Table 1) that depend on the value of the cyclic stress amplitude. As suggested by François et
 242 al. [49], the model parameters need to be determined by nonlinear least squares method.
 243 Detailed values of the model parameters can be found in Table 1.

244

245

VI. MODEL PERFORMANCE

246 It was found that the stress amplitude had significant influence on the cyclic deformation
 247 of granular soils in the long run [8-10]. To validate the proposed mathematical model, test
 248 results of four different granular soils, as shown in Table 2, are used. The natural quartz sand
 249 was taken from a sand pit near Dorsten, Germany [10]. The grain shape is sub-angular and
 250 the specific weight along with the other physical properties can be found in Table 2. The
 251 samples were tested under different drained cyclic triaxial loading conditions with the
 252 averaged mean principal stress equal 200 kPa and the averaged deviator stresses equal to 50
 253 kPa, 100 kPa, 150 kPa, 175 kPa, and 225 kPa. Each loading condition had the same cyclic
 254 stress amplitude q^{ampl} , equal to 40 kPa, and the same loading frequency, equal to 1 Hz. Fig. 7

255 shows the model simulation of the cumulative deformations of natural quartz sand [10]. The
256 cumulative strain increased with the increase of the applied average stress ratio. It is observed
257 that the mathematical model can well capture both the long-term shear strain and volumetric
258 strain under different deviator stresses. It can also give satisfactory predictions of the initial
259 deformations for several test conditions. However, if more different complicated loading
260 conditions involved, this model indeed loses some ability in accurately predicting the
261 deformation at the initial loading stage, for example, test result with higher stress ratio. This
262 is because this model aims at predicting the long-term cumulative deformation rather than the
263 short-term stress strain response of the sample. However, this shortcoming can be resolved by
264 using variable fractional derivative order but is not within the scope of current research. To
265 the author's knowledge, the fractional derivative order could depend on the mechanical state,
266 such as the loading stress and strain, etc. [27-29]. But, the use of the variable order may
267 involve significantly complex mathematic calculations (see [27] for instance), which is not
268 applicable for the engineering concern. The predictions of the numerical model, denoted as
269 François model [46], are also provided for comparison. As shown in Fig. 7, it can only give
270 comparatively good predictions of the soil deformation under low stress ratios. In contrast,
271 the proposed model exhibits better potential in characterising the cumulative deformation of
272 the natural quartz sand under both low and high stress ratios.

273 The railroad ballast was a kind of crushed basalt, collected from Bombo quarry near
274 Wollongong, New South Wales, Australia. It was an angular/subangular volcanic latite basalt
275 that contains the primary minerals feldspar, plagioclase, and augite [42]. Its physical
276 attributes can be found in Table 2. The railroad ballast was tested under the confining
277 pressures equal to 10 kPa, 60 kPa, 120 kPa with two different cyclic stress amplitudes equal
278 to 185 kPa and 455 kPa. The sample was prepared by tamping to 300 mm in diameter and
279 600 mm in height before tested under a loading frequency equal to 20 Hz. Fig. 8 shows the
280 comparison between the test results and the predicted results by the proposed model as well
281 as the François model. It is observed from Fig. 8(a) that the proposed model can well capture
282 the cumulative shear strain of ballast tested under different confining and deviator stresses.
283 The cumulative shear strain increased with increasing confining pressure. Larger deviator
284 stress resulted in larger cumulative shear strain given the same confining pressure. Moreover,
285 through the incorporation of the modified cyclic flow rule, the proposed model can well
286 characterize both the volumetric dilatancy under low confining pressure and the volumetric
287 contraction under relatively high confining pressure, as shown in Fig. 8(b). But in contrast,
288 the François model can only give satisfactory predictions of the shear strains under low
289 confining pressure and the volumetric strains under high confining pressure. Most
290 importantly, the model parameters are highly dependent on the cyclic amplitude. Therefore,
291 the proposed model exhibits a better flexibility in modelling the long-term deformation of
292 different granular soils tested under different loading conditions.

293 Moreover, to preliminarily demonstrate the ability of the fractional order model in
294 characterising the entire stress strain hysteresis curve, two additional cyclic tests, as shown in
295 Figs. 9 and 10, are simulated by using Eq (7). Fig. 9 shows the prediction of the drained
296 cyclic triaxial tests on the Zipingpu rockfill [14]. The sample was prepared to have a diameter

297 equal to 300 mm and a height equal to 600 mm before initially compressed to an effective
298 mean principal stress equal to 500 kPa. The subsequent test was conducted under the stress
299 amplitude equal to 400 kPa. The physical properties of the sample can be found in Table 2.
300 The shear-related moduli, G_0 , used for first, second loading and the subsequent unloading are
301 15.5 MPa, 9.7 MPa, 7.0 MPa, respectively. The compression-related moduli, K_0 , used for first,
302 second loading and the subsequent unloading are 42.3 MPa, 5.5 MPa, and 1.0 MPa,
303 respectively. The fractional order α is found to be 0.71. It is observed from Fig. 9(a) that the
304 proposed approach can well represent the virgin loading and unloading of the Zipingpu
305 rockfill. The subsequent hysteresis loops between the axial strain and the deviator stress can
306 be also characterised. However, as shown in Fig. 9(b), the proposed model can only simulate
307 the increase of the volumetric strain during virgin loading. The subsequent variation cannot
308 be well simulated. Fig. 10 shows the prediction of the triaxial test results performed on a dense
309 rockfill [22] which consisted of mainly weathered quartz monzonite. The triaxial test was
310 performed on a 300 mm diameter and 700 mm high specimen. The initial effective mean
311 principal stress was equal to 3 MPa and the subsequent loading amplitude was 2MPa with a
312 loading frequency equal 0.1 Hz. Detailed physical properties of the Toyoura sand can be
313 found in Table 2. The shear-related moduli, G_0 , used for first, second loading and the
314 subsequent unloading are 32 MPa, 7.1 MPa, 9.5 MPa, respectively. The compression-related
315 moduli, K_0 , used for first, second, loading and the subsequent unloading are 5.82 MPa, 4.0
316 MPa, and 0.58 MPa, respectively. The fractional order $\alpha = 0.81$. Once again, a well
317 representation of the stress strain hysteresis can be observed from Fig. 10(a). But the
318 predicted volumetric strain is relatively higher than the experimental results. Further
319 modification of the current model needs to be conducted in order to accurately capture the
320 variation of the volumetric strain during cyclic loading.

321

322

VII. CONCLUSIONS

323 A fractional order model was presented to simulate the cumulative deformation of
324 granular soils subjected to cyclic loading. This model consists of two main parts. Firstly, a
325 fractional derivative was used to derive the power law connection between the cumulative
326 shear strain and its loading cycles. Then, an energy based approach was employed to provide
327 a modified cyclic flow rule particularly for crushable granular soils. The modified the flow
328 rule took into account the particle breakage of granular soils under cyclic loading thus had a
329 better potential in characterizing the cyclic flow direction of granular soils. All the model
330 parameters can be determined from the cyclic and static triaxial tests. It is noted that the
331 physical origins of several parameters are not clear and still need further investigation. To
332 validate the proposed model, predicted and measured results for several different granular
333 soils, i.e., sand, rockfill, and railroad ballast, were simulated. The proposed model was also
334 compared with an existing cumulative model to demonstrate its advantage in modelling long-
335 term deformation of granular soils. It was observed that with the help of the fractional
336 derivative theory, the distinct power law evolution between the shear strain and the
337 corresponding loading cycle under different loading conditions was reasonably captured.
338 Besides, by employing the modified cyclic flow rule, the model was also able to predict both

339 the volumetric compression under relatively high confining pressure and the volumetric
340 dilatancy under low confining pressure. It is thus concluded that the proposed model could
341 well capture both the cumulative shear strain and the cumulative volumetric strain of granular
342 soils. Moreover, to preliminary demonstrate the fractional order approach in modelling the
343 stress strain hysteresis during cyclic loading, two additional simulations of the triaxial test
344 results performed on rockfill were also provided. The fractional order approach was shown to
345 have great potential in modelling the entire stress and strain curve of rockfill during cyclic
346 loading. However, this model cannot accurately represent the variation of the volumetric
347 deformation. Further modifications still need be conducted.

348

349

ACKNOWLEDGEMENTS

350 The authors would like to thank Professor W. Chen and Dr Xiaodi Zhang in Hohai
351 University for their kind instructions on several fundamentals of the fractional calculus. The
352 financial supports provided by the Fundamental Research Funds for the Central Universities
353 (Grant No. 106112015CDJXY200008) is also greatly appreciated.

354

355

REFERENCES

- 356 [1] Miura,N., Fujikawa,K., Sakai,A. and Hara,K. Field measurement of settlement in saga
357 airport highway subjected to trafficload. *Tsuchi-to-Kiso*, 1995, 43-6(449): 49–51.
- 358 [2] Ren,X.W., Tang,Y.Q., Li,J. and Yang,Q. A prediction method using grey model for
359 cumulative plastic deformation under cyclic loads. *Natural Hazards*, 2012, 64(1): 441–457.
- 360 [3] Li,D.Q. and Selig,E.T. Cumulative plastic deformation for fine grained subgrade soils.
361 *Journal of Geotechnical Engineering ASCE*, 1996, 122(12): 1006–1013.
- 362 [4] Chai,J.C. and Miura,N. Traffic-load-induced permanent deformation of road on soft
363 subsoil. *Journal of Geotechnical and Geoenvironmental Engineering*, 2002, 128(11): 907–
364 916.
- 365 [5] Bouckovalas,G., Whitman,R.V. and Marr,W.A. Permanent displacement of sand with
366 cyclic loading. *Journal of Geotechnical Engineering ASCE*, 1984, 110(11): 1606–1623.
- 367 [6] Suiker,A.S.J. and de,Borst,R. A numerical model for the cyclic deterioration of railway
368 tracks. *International Journal for Numerical Methods in Engineering*, 2003, 57(4), 441–
369 470.
- 370 [7] Khalili,N., Habte,M. and Valliappan,S. A bounding surface plasticity model for cyclic
371 loading of granular soils. *International Journal for Numerical Methods in Engineering*,
372 2005, 63(14), 1939–1960.
- 373 [8] Niemunis,A., Wichtmann,T. and Triantafyllidis,T.H. A high-cycle accumulation model for
374 sand. *Computer and Geotechnics*, 2005, 32(4): 245–263.
- 375 [9] Wichtmann,T., Niemunis,A. and Triantafyllidis,T.H. Experimental evidence of a unique
376 flow rule of non-cohesive soils under high-cyclic loading. *Acta Geotechnica*, 2006, 1(1):
377 59–73.

- 378 [10] Wichtmann,T., Niemunis,A. and Triantafyllidis,T.H. Validation and calibration of a high-
379 cycle accumulation model based on cyclic triaxial tests on eight sands. *Soils and*
380 *Foundations*, 2009, 49(5), 711–728.
- 381 [11] Li,S., and Huang,M. Undrained long-term cyclic degradation characteristics of offshore
382 soft clay. *In Proceedings of the GeoShanghai 2010 International Conference, Shanghai,*
383 *China. Huang M S, Yu X, Huang Y, eds. 2010. 263–271.*
- 384 [12] Li,L.L., Dan,H.B. and Wang,L. Z. Undrained behavior of natural marine clay under cyclic
385 loading, *Ocean Engineering*, 2011, 38(16): 1792–1805.
- 386 [13] Karim,M.R., Oka,F., Krabbenhoft,K., Leroueil,S. and Kimoto,S. Simulation of long-term
387 consolidation behavior of soft sensitive clay using an elasto-viscoplastic constitutive
388 model. *International Journal for Numerical and Analytical Methods in Geomechanics*,
389 2013, 37(16): 2801–2824.
- 390 [14] Liu,H., Zou,D. and Liu,J. Constitutive modeling of dense gravelly soils subjected to cyclic
391 loading. *International Journal for Numerical and Analytical Methods in Geomechanics*,
392 2014, DOI: 10.1002/nag.2269.
- 393 [15] Seidalinov,G. and Taiebat,M. Bounding surface SANICLAY plasticity model for cyclic
394 clay behavior. *International Journal for Numerical and Analytical Methods in*
395 *Geomechanics*, 2014, 38(7): 702–724.
- 396 [16] Ishikawa,T., Sekine,E. and Miura,S. Cyclic deformation of granular material subjected to
397 moving-wheel loads. *Canadian Geotechnical Journal*, 2011, 48(5): 691–703.
- 398 [17] Suiker,A.S.J, Selig,E.T. and Frenkel,R. Static and cyclic triaxial testing of ballast and
399 subballast. *Journal of Geotechnical and Geoenvironmental Engineering*, 2005, 131(6):
400 771–782.
- 401 [18] Indraratna,B., Lackenby,J. and Christie,D. Effect of confining pressure on the degradation
402 of ballast under cyclic loading. *Géotechnique*, 2005, 55(4): 325–328.
- 403 [19] Lackenby,J., Indraratna,B., McDowell,G. and Christie,D. Effect of confining pressure on
404 ballast degradation and deformation under cyclic triaxial loading. *Géotechnique*, 2007,
405 57(6): 527–536.
- 406 [20] Indraratna,B., Thakur,P.K. and Vinod,J.S. Experimental and numerical study of railway
407 ballast behavior under cyclic loading. *International Journal of Geomechanics*, 2009, 10(4):
408 136–144.
- 409 [21] Xiao,Y., Liu,H., Chen,Y. and Jiang,J. Bounding surface model for rockfill materials
410 dependent on density and pressure under triaxial stress conditions. *Journal of Engineering*
411 *Mechanics*, 2014, 140(4), 04014002. doi: 10.1061/(ASCE)EM.1943-7889.0000702.
- 412 [22] Fu,Z., Chen,S. and Peng,C. Modeling cyclic behavior of rockfill materials in a framework
413 of generalized plasticity. *International Journal of Geomechanics*, 2014, 14(2): 191–204.
- 414 [23] Ling,H.I. and Yang,S. Unified sand model based on the critical state and generalized
415 plasticity. *Journal of Engineering Mechanics*, 2006, 132(12): 1380–1391.
- 416 [24] Indraratna,B., Thakur,P.K., Vinod,J.S. and Salim,W. Semi-empirical cyclic densification
417 model for ballast incorporating particle breakage. *International Journal of Geomechanics*,
418 2012, 12(3): 260–271.
- 419 [25] Chrimer,S. and Selig,E.T. Computer model for ballast maintenance planning. *In*
420 *Proceedings of 5th International Heavy Haul Railway Conference, Beijing, China. 1993,*
421 *223–227.*

- 422 [26] Indraratna,B., Salim,W., Ionescuc,D. and Christie,D. Stress-strain and degradation
423 behavior of railway ballast under static and dynamic loading, based on large-scale triaxial
424 testing. *In Proceedings of 15th international conference on soil mechanics and*
425 *geotechnical engineering, Istanbul, Turkey, 2001, 2093–2096.*
- 426 [27] Sun,H.G., Chen,W. and Chen,Y.Q. Variable-order fractional differential operators in
427 anomalous diffusion modeling, *Physica A*, 2009, 388(21): 4586–4592.
- 428 [28] Sun,Y., Liu,H., Xiao,Y. Gao,H. and Cui,Y. Modeling of rheological behavior of
429 geomaterials based on fractional viscoelastic equation with variable parameters. *In*
430 *Proceedings of GeoHunan international conference 2011, Hunan, China. Ge L, Zhang X,*
431 *Wu J, Correia A G, eds. 2011. 107–114.*
- 432 [29] Yin,D., Wu,H., Cheng,C. and Chen,Y.Q. Fractional order constitutive model of
433 geomaterials under the condition of triaxial test. *International Journal for Numerical and*
434 *Analytical Methods in Geomechanics*, 2013, 37(8): 961–972.
- 435 [30] Yin,D., Duan,X. and Zhou,X. Fractional time-dependent deformation component models
436 for characterizing viscoelastic Poisson's ratio. *European Journal of Mechanics A/Solids*,
437 2013, 42: 422–429.
- 438 [31] Kilbas,A.A.A, Srivastava,H.M. and Trujillo,J.J. Theory and applications of fractional
439 differential equations. Elsevier Science Limited, 2006. 91–99.
- 440 [32] Rowe,P.W. The stress-dilatancy relation for static equilibrium of an assembly of particles
441 in contact. *Proceedings of Royal Society of London A Mathematical and Physical Science*,
442 1962, 269(1339): 500–527.
- 443 [33] Indraratna,B. and Salim,W. Modelling of particle breakage of coarse aggregates
444 incorporating strength and dilatancy. *Proceedings of ICE Geotechnical Engineering*, 2002,
445 155(4): 243–252.
- 446 [34] Sun,Y., Liu,H. and Yang,G. Yielding function for coarse aggregates considering gradation
447 evolution induced by particle breakage. *Rock and Soil Mechanics*, 2013, 34(12): 3479–
448 3484.
- 449 [35] Liu,H., Sun,Y., Yang,G. and Chen,Y. A review of particle breakage characteristics of
450 coarse aggregates. *Journal of Hohai University (Natural Sciences)*. 2012, 40(4): 361–369.
451 (in Chinese).
- 452 [36] McDowell,G.R. A family of yield loci based on micro mechanics. *Soils and Foundations*,
453 2000, 40(6): 133–137.
- 454 [37] Chang,C.S and Whitman,R.V. Drained permanent deformation of sand due to cyclic
455 loading. *Journal of Geotechnical Engineering ASCE*, 1988, 114(10): 1164–1180.
- 456 [38] Wichtmann,T., Niemunis,A.and Triantafyllidis,T.H. Flow rule in a high-cycle
457 accumulation model backed by cyclic test data of 22 sands. *Acta Geotechnica*, 2014, 1–15.
- 458 [39] Richart,F.E.Jr, Hall,J.R. and Woods,R.D. Vibrations of soils and foundations. Englewood
459 Cliffs, NJ: Prentice-Hall, 1970.
- 460 [40] Li,X. and Dafalias,Y. Dilatancy for cohesionless soils. *Géotechnique*, 2000, 50(4), 449–
461 460.
- 462 [41] Li,D. and Selig,E.T. Cumulative plastic deformation for fine-grained subgrade soils.
463 *Journal of Geotechnical Engineering ASCE*, 1996, 122(12): 1006–1013.

- 464 [42] Lackenby, J. Triaxial behaviour of ballast and the role of confining pressure under cyclic
465 loading. Dissertation for the Doctoral Degree. Wollongong: University of Wollongong,
466 2006. 89–91.
- 467 [43] Xiao, Y., Liu, H., Chen, Y., Jiang, J., and Zhang, W. State-dependent constitutive model for
468 rockfill materials. *International Journal of Geomechanics*, 2014, 04014075. doi:
469 10.1061/(ASCE)GM.1943-5622.0000421.
- 470 [44] Indraratna, B., Wijewardena, L.S.S. and Balasubramaniam, A.S. Large-scale triaxial testing
471 of greywacke rockfill. *Géotechnique*, 1993, 43(1), 37–51.
- 472 [45] Frossard, E., Dano, C., Hu, W., and Hicher, P.Y. Rockfill shear strength evaluation: a
473 rational method based on size effects. *Géotechnique*, 2012, 62(5), 415–427.
- 474 [46] Xiao, Y., Liu, H., Chen, Y., and Jiang, J. Bounding Surface Plasticity Model Incorporating
475 the State Pressure Index for Rockfill Materials. *Journal of Engineering Mechanics*, 2014,
476 140(11), 04014087. doi: 10.1061/(ASCE)EM.1943-7889.0000802.
- 477 [47] Xiao, Y., Liu, H., Chen, Y., Jiang, J. and Zhang, W. Testing and modeling of the state-
478 dependent behaviors of rockfill material. *Computers and Geotechnics*, 61(9), 153–165.
- 479 [48] Xiao, Y., Sun, Y., and Hanif, F. A particle-breakage critical state model for rockfill material.
480 *Science China Technological Sciences*, 58(7), 1125-1136.
- 481 [49] François, S., Karg, C., Haegeman, W., and Degrande, G. A numerical model for foundation
482 settlements due to deformation accumulation in granular soils under repeated small
483 amplitude dynamic loading. *International Journal for Numerical and Analytical Methods
484 in Geomechanics*, 2010, 34(3): 273-296.
- 485

Table caption list:

Table 1 Model parameters

Table 2 Physical properties of the granular soils

Table 1. Model parameters

Model	Parameters	Natural quartz sand [10]	Railroad ballast [42]		
Current model	q^{ampl} (kPa)	40	185	455	
	G_0 (kPa)	230	383	383	
	K_0 (kPa)	213	355	355	
	M	1.28	4.66	4.66	
	b	0	0.82	0.82	
	a	1.64	1.8	1.8	
	α	0.15	0.1	0.1	
	β	0.55	1.0	1.0	
	D	1477.34	318.8	318.8	
	m	0.56	-1.1	-1.1	
	n	-0.21	-0.72	-0.72	
	François model [49]	$\alpha_f (10^{-4})$	0.007	7.4	2.6
		$\beta_f (10^{-6})$	-0.07	-5.4	-21.8
η_f		700	105.9	7.0	
d_f		0.25	0.01	0.01	
$\alpha_c (10^{-4})$		0.04	8.0	0.56	
$\beta_c (10^{-6})$		-0.02	-78	-3.4	
η_c		700	1.1	85.7	
$C_p (\text{Pa}^{-1})$		0.005	0.007	0.007	
K_{ref}		213	355	355	
ν		0.2	0.2	0.2	

Table 2. Physical properties of the granular soils

Materials	Natural quartz sand [10]	Zipingpu rockfill [14]	Weathered monzonite [22]	Railroad ballast [42]
G_s	2.65	-	2.71	2.66
d_{50} (mm)	0.35	9.5	18	39.5
C_u	1.9	-	11	1.53
e_{max}	0.930	-	0.3	0.97
e_{min}	0.544	-	0.15	0.67
e_0	0.745	0.313	0.17	0.74

Figure caption list:

Fig. 1. Schematic representation of the cyclic triaxial test

Fig. 2. Cyclic flow rule

Fig. 3. Critical state line and peak stress line

Fig. 4. Determination of parameters a and β

Fig. 5. Determination of exponent α

Fig. 6. Determination of parameters D , m and n

Fig. 7. Model predictions of the cumulative deformation of natural quartz sand [10]

Fig. 8. Model predictions of the cumulative deformation of railroad ballast [42]

Fig. 9. Representation of the stress strain behaviour of Zipingpu rockfill [14]

Fig. 10. Representation of the stress strain behaviour of weathered monzonite [22]

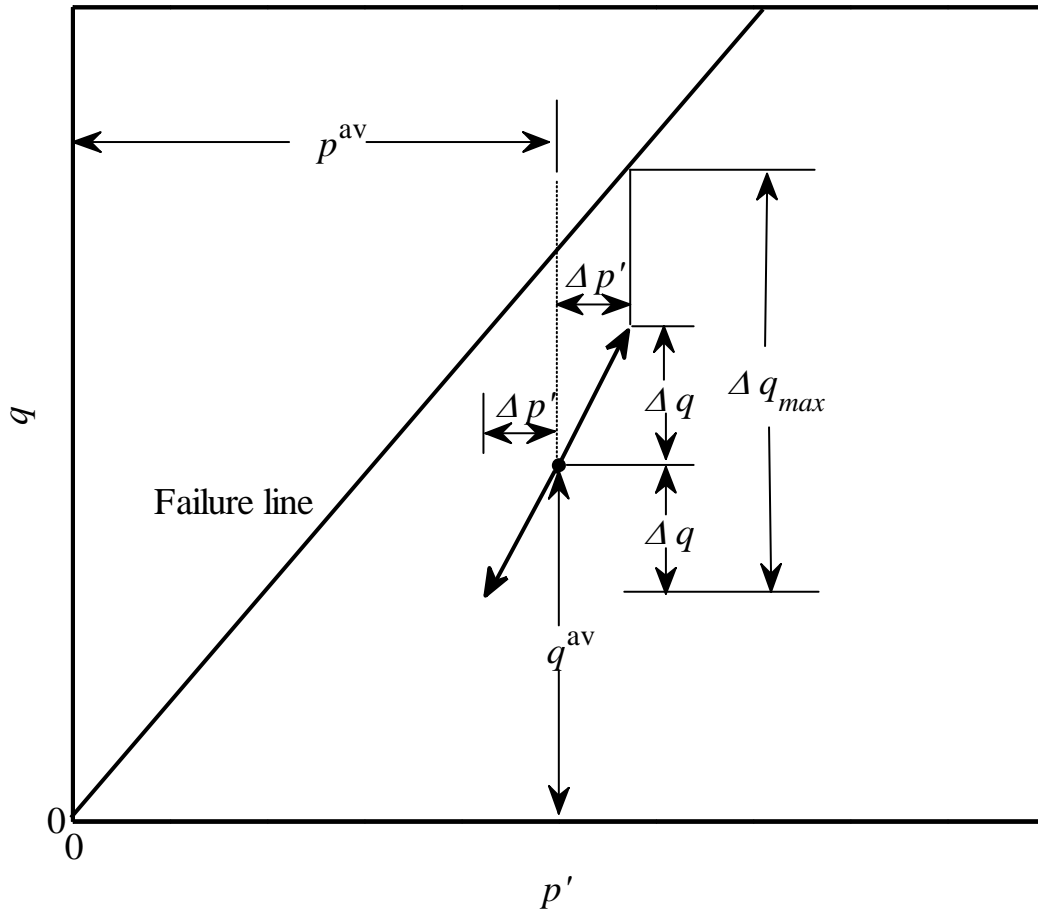


Fig. 1. Schematic representation of the cyclic triaxial test

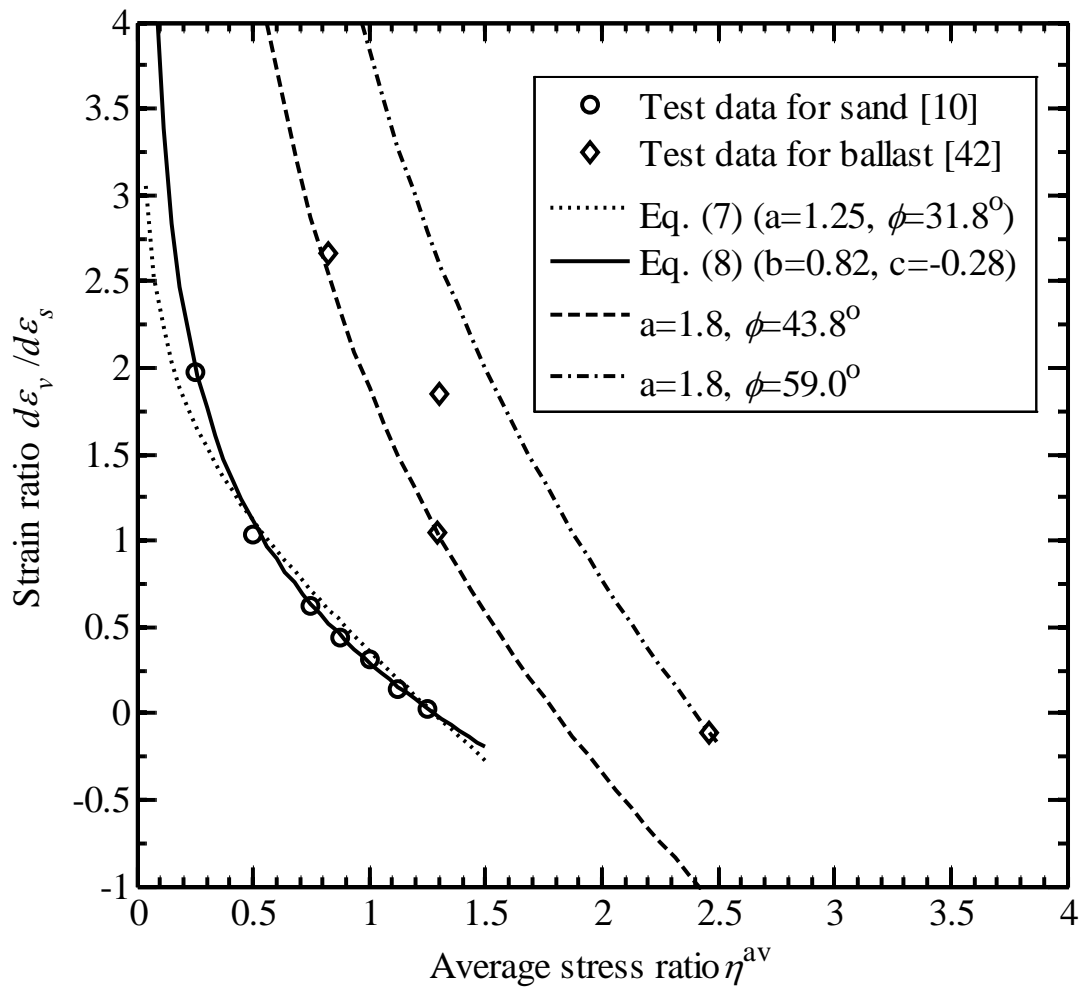


Fig. 2. Cyclic flow rule

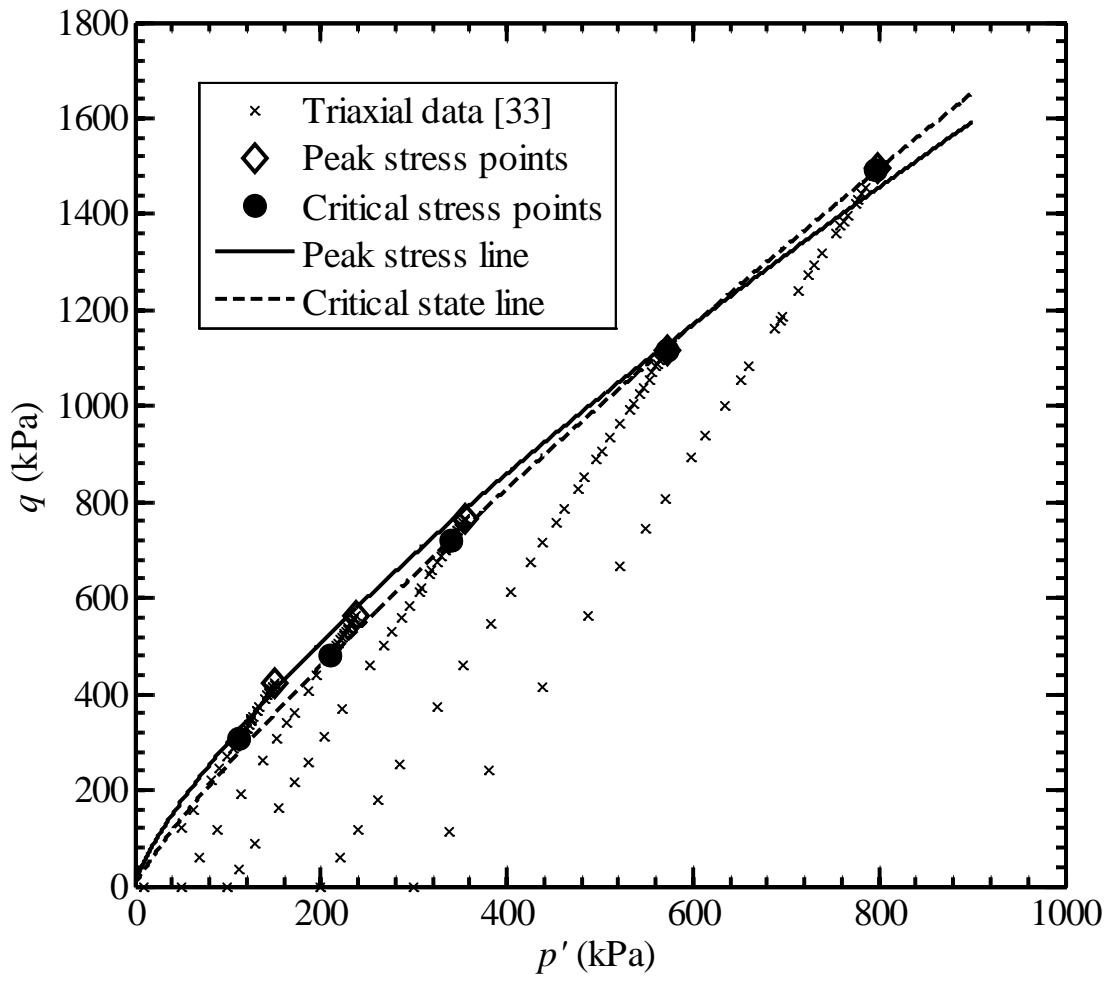


Fig. 3. Critical state line and peak stress line

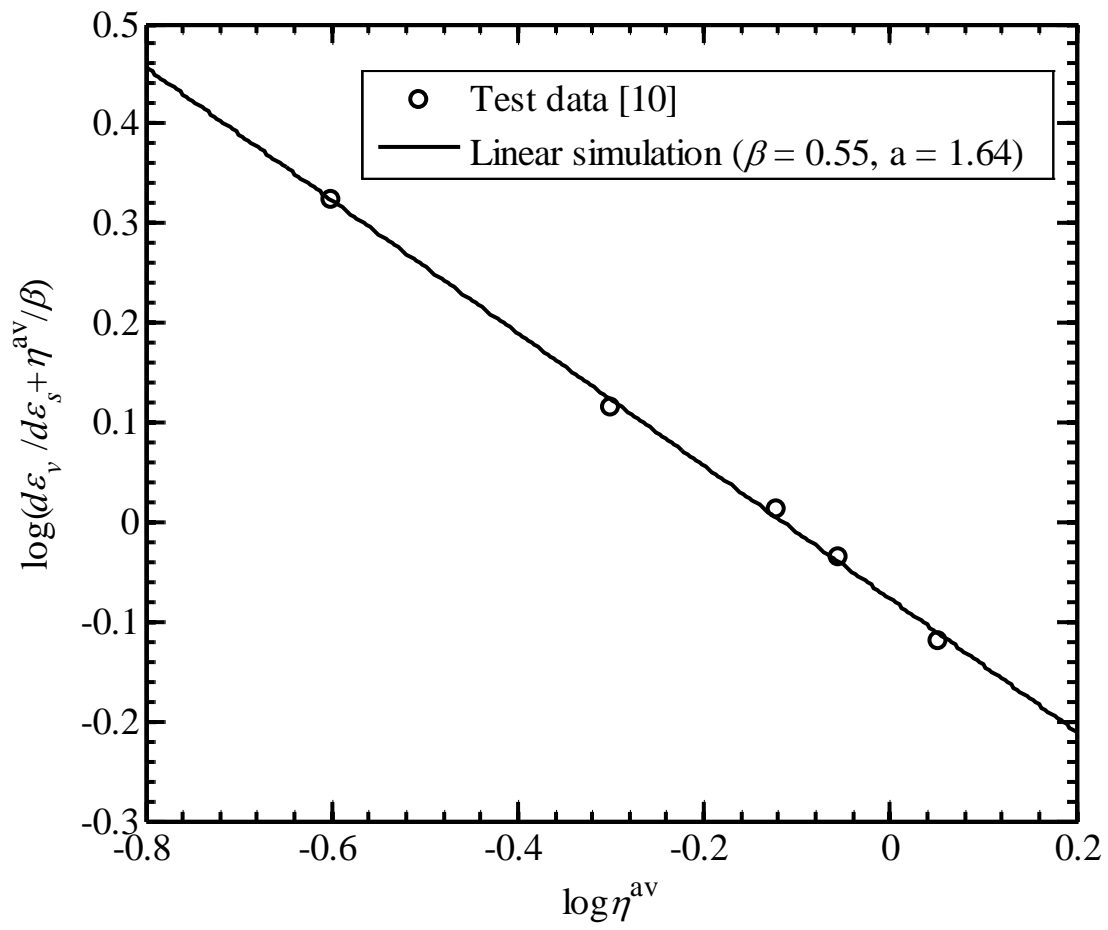


Fig. 4. Determination of parameters a and β

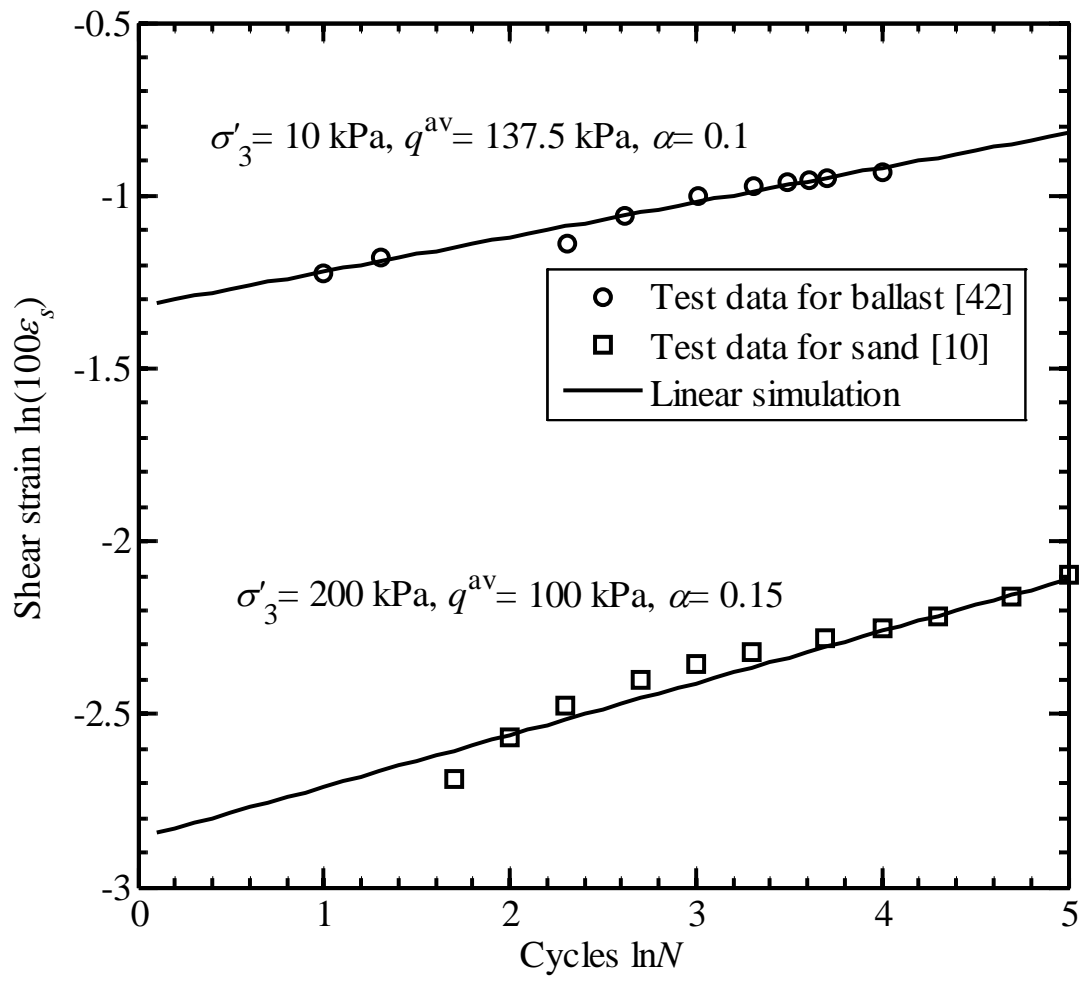


Fig. 5. Determination of exponent α

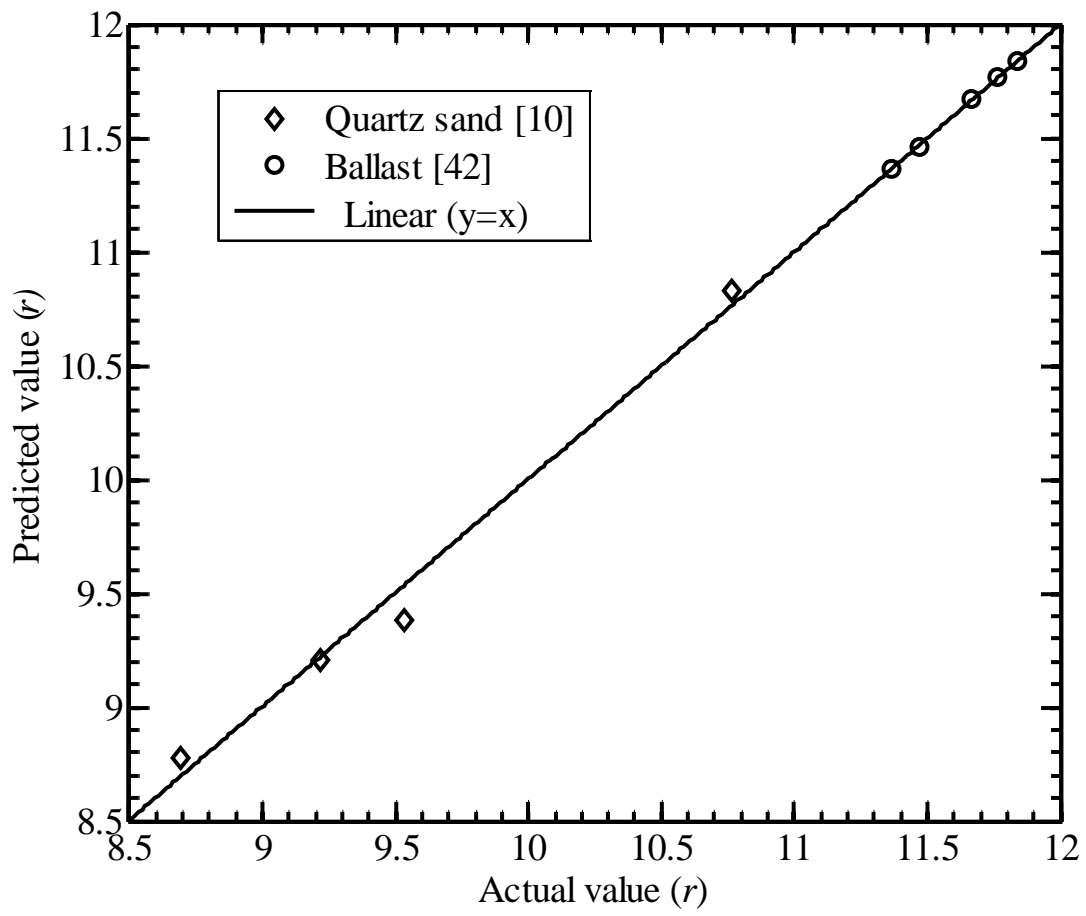


Fig. 6. Determination of parameters D , m and n

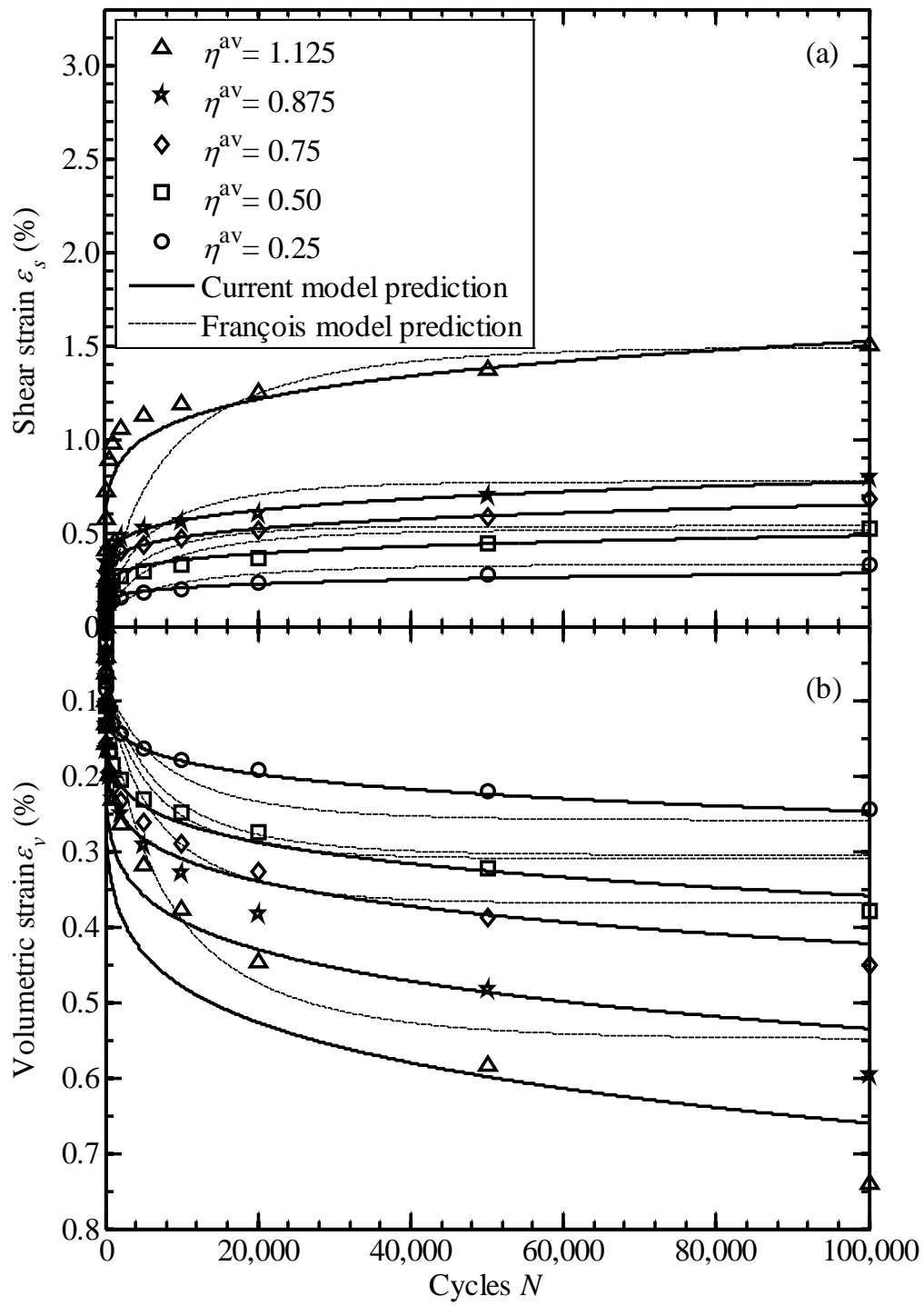


Fig. 7. Model predictions of the cumulative deformation of natural quartz sand [10]

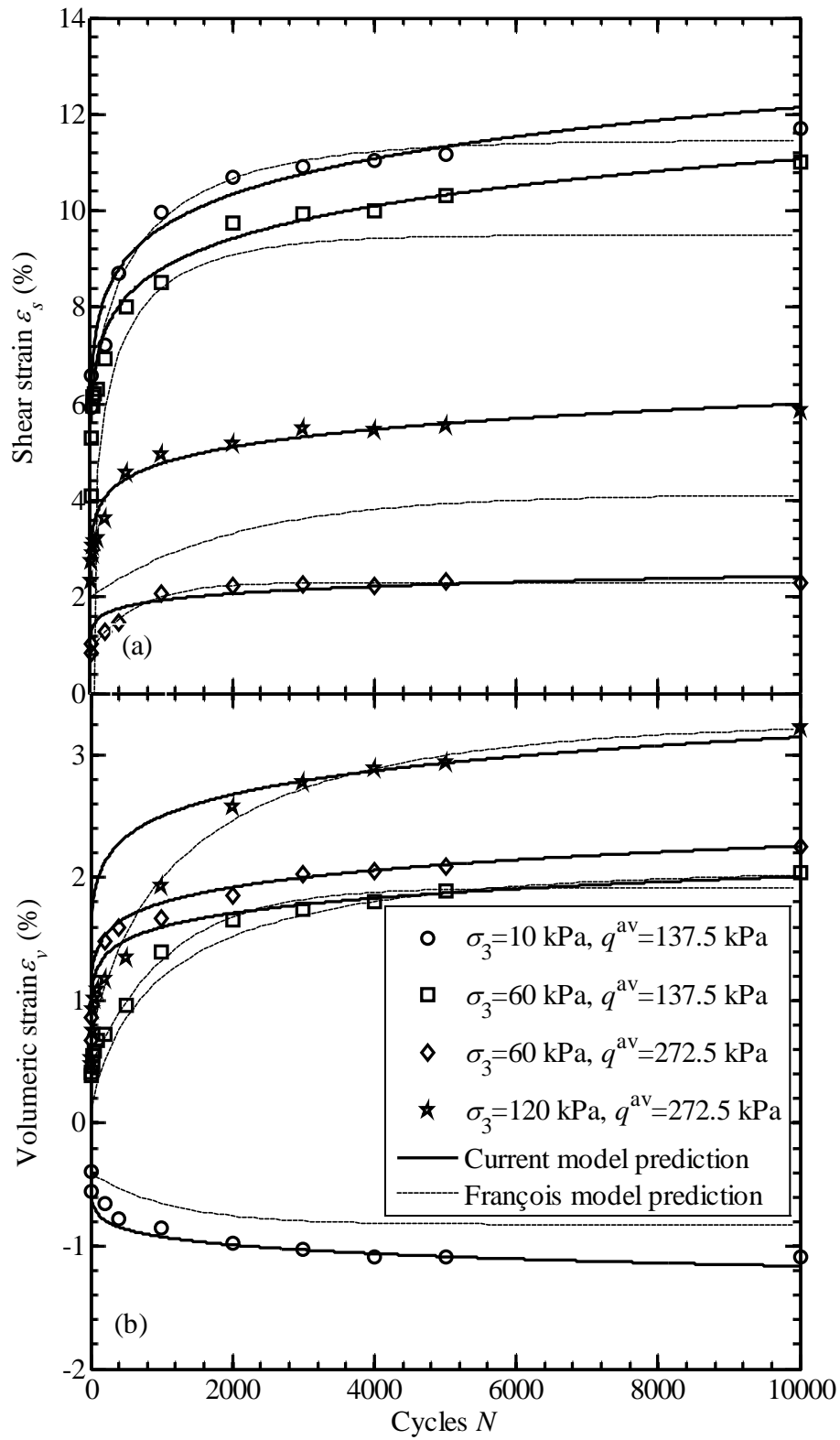


Fig. 8. Model predictions of the cumulative deformation of railroad ballast [42]

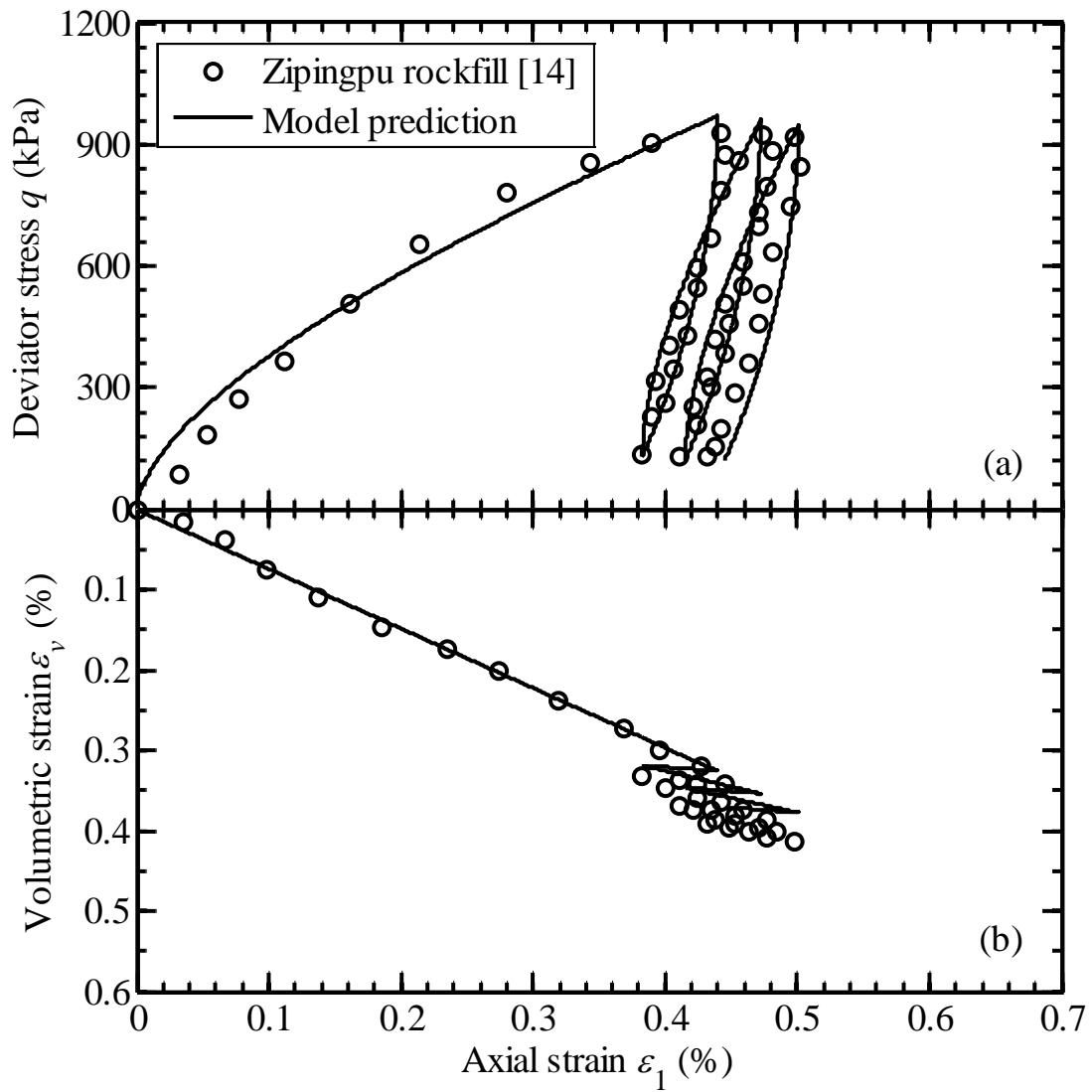


Fig. 9. Representation of the stress strain behaviour of Zipingpu rockfill [14]

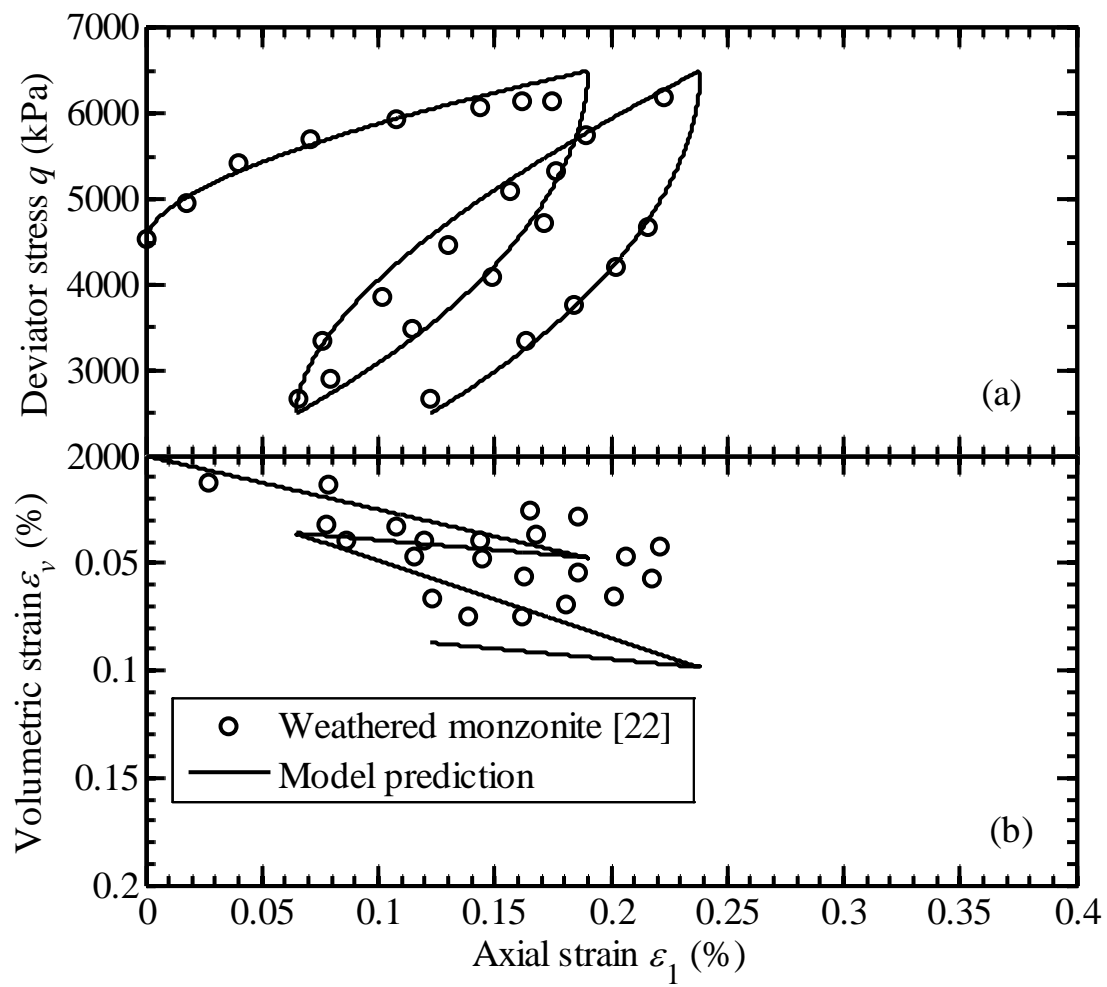


Fig. 10. Representation of the stress strain behaviour of weathered monzonite [22]